DISCRETE ELEMENT MODELING AND PARAMETER CALIBRATION OF THE WHEAT ROOT–SOIL COMPOSITE
/
小麦根土复合体离散元模型建立与标定试验

Chengcheng GUO[1)], Zhiping YANG*[1)], Junchang ZHANG[2)], Huiyan YIN[1)], Cui LI[1)]
[1)]College of Agricultural Machinery and Automotive Engineering, Gansu Polytechnic College of Animal Husbandry & Engineering, Wuwei 733006/ China;
[2)]College of Mechanical and Electronic Engineering, Northwest A&F University, Yangling 712100/ China;
Tel: +86 18729219567; E-mail: 1091257144@qq.com
DOI: https://doi.org/10.35633/inmateh-79-72

Keywords: *root-soil composite, conservation tillage, discrete element method, shear test, parameter calibration*

ABSTRACT
Due to the anisotropy and small size of wheat roots, as well as the neglect of shear process effects on mechanical properties in existing wheat root-soil composite (WRSC) models, the establishment and parameter calibration of WRSC models remain inaccurate, hindering the precise analysis of the microscopic effects of furrow openers on WRSC during no-till sowing. This study aimed to develop an accurate and reliable WRSC model based on the discrete element method (DEM) using rapid particle filling and the Hertz-Mindlin with bonding contact model. Plackett-Burman tests identified particle shear modulus, inter-particle bonding radius, and bonding stiffness as significant factors affecting the ultimate shear force of wheat roots. Steepest ascent tests narrowed the optimal parameter ranges, and Box-Behnken test results were used to establish a quadratic regression model, leading to the optimal parameter combination: particle shear modulus of 7.96 MPa, inter-particle bonding stiffness of 4.13 GN/m³, and bonding radius of 0.32 mm. Actual and simulated shear tests on WRSC were conducted, and key parameters between wheat roots and soil particles were calibrated via steepest ascent tests with the ultimate shear force on the cutter as the target value: static friction coefficient of 0.8, bonding stiffness of 11 MN/m³, and critical stress of 11 MPa. Validation showed a relative error of 7.35% between simulated and actual shear resistance, indicating that the proposed WRSC model and parameters can effectively simulate field operations such as furrowing and rotary tillage.

摘要
针对玉米免耕播种时前茬小麦根系与开沟器相互作用过程分析复杂，且小麦根系的各向异性和直径较小等特点，现有根土复合体模型忽略小麦根系对对剪切过程力学特性的影响导致标定参数不准确的问题，该研究基于离散元法采用颗粒快速填充和 Hertz-Mindlin with bonding 粘结模型建立了一种准确性和可靠性较高的小麦根-土复合体模型。基于 Hertz-Mindlin bonding 粘结模型，采用颗粒快速填充的方法，构建小麦根系模型。通过 Plackett-Burman 试验发现颗粒剪切模量和颗粒间粘结半径、粘结刚度对小麦根系极限剪力有显著影响。通过最陡爬坡试验确定显著性影响参数最优区间的基础上，根据 Box-Behnken 试验结果建立了根系极限剪力与显著性影响参数的二阶回归模型并对其进行优化，得到显著性参数的最佳组合为：颗粒剪切模量 7.96 MPa、颗粒间粘结刚度 4.13 GN/m3、粘结半径 0.32 mm。其次，采用最陡爬坡试验方法，标定了小麦根-土间的关键参数。以切刀受到的极限剪力为目标值，基于小麦根-土复合体进行实际剪切和仿真剪切试验结果，标定得到小麦根系与土壤颗粒间的静摩擦系数为 0.8、粘结刚度为 11 MN/m3、临界应力为 11 MPa。最后，验证标定后的根-土复合体模型，结果显示仿真剪切阻力与实际剪切阻力间相对误差为 7.35%，表明基于离散元法建立的小麦根-土复合体模型可以用于模拟田间实际土壤环境。

INTRODUCTION
Conservation tillage is an important agricultural technology for improving soil quality, conserving water and moisture, and enhancing economic benefits. As a key link in conservation tillage, no-till and reduced-till sowing imposes higher requirements on the performance of furrow openers.

In the double cropping area of Guanzhong, Shaanxi Province, corn no-till sowing is carried out immediately after wheat harvest. Undecomposed wheat roots in the soil are closely bonded with soil particles, significantly increasing the working resistance of furrow openers and intensifying soil disturbance.

Traditional soil bin tests fail to reflect the actual field operating environment due to the absence of root factors, while the discrete element method provides an effective means to simulate complex root-soil interactions.

Yang et al. (1996) first explicitly proposed the concept of "soil-root composite" in their study on herbaceous plant roots. Since roots are tightly attached to soil, they reinforce soil structure and improve water absorption capacity. The combination of crop roots and soil is termed the root-soil composite, and it is assumed to partially satisfy the Mohr-Coulomb law. Currently, experimental methods are mainly used to study the shear resistance of root-soil composites. However, numerous factors influence shear resistance, broadly categorized into soil-related and plant root-related factors *(Chen et al., 2026)*, each encompassing multiple sub-factors. Consequently, experimental studies on composite shear resistance are labor-intensive and time-consuming. The discrete element method is a numerical computation technique for analyzing complex dynamic discrete systems, with distinct advantages in agricultural machinery research. With advancements in computer hardware and DEM theory, numerical simulation has been increasingly applied to study root-soil interactions due to its higher efficiency, season independence, and low cost *(Ji et al., 2012; Yang et al., 2014; Ji et al., 2014; Tian et al., 2015)*. Yang et al. established a soil model using DEM and a rigid lettuce root model via SolidWorks. However, their pull-out simulations failed to account for root deformation and bending, leading to significant discrepancies between simulated and actual results. *Lenaerts et al. (2014)*, *Li et al. (2016)*, and *Gao et al. (2020)* respectively established slender straw models using DEM, but the minimum particle units employed prevented cutting and separation. *Li et al. (2020)* and *Liu et al. (2018)* successfully developed flexible corn and spinach root models capable of bending and fracture using the Hertz-Mindlin with bonding model and rapid particle filling. To date, no literature has been published on the establishment of a wheat root-soil composite DEM model. Wheat roots differ significantly from corn and spinach roots in diameter and mechanical properties, necessitating the development of a dedicated DEM model for wheat root-soil composites.

To address the aforementioned issues, this study determined the morphological dimensions of wheat root models by analyzing the actual growth state of wheat roots in post-harvest soil, and constructed a complete flexible wheat root model using EDEM. Parameters of wheat roots, soil, and their interactions were calibrated through comparative validation of actual and simulated tests, aiming to improve the accuracy of the wheat root-soil composite DEM model. This research provides a foundation and reference for the establishment of DEM models for wheat root-soil composites and similar agricultural materials.

MATERIALS AND METHODS

Physical Properties of Materials

Physical Parameters of Wheat Roots

Roots of the wheat cultivar "Xinong 511" were sampled from the experimental field of Northwest A&F University on June 2, 2025. The experimental field was regularly fertilized prior to planting, meeting standard cultivation conditions, with manual weeding performed during the growing period before harvest the following year. A wheat-growing area of 1.5 m × 1.3 m (6 rows) was selected for statistical counting. Field investigations revealed that wheat grows in clusters with an inter-cluster spacing of 30 mm (Fig. 1).

Fig. 1 - Wheat growth status

Five clusters of wheat roots were collected using the five-point sampling method (Fig. 2a). Each cluster contained an average of 20 roots, which were twisted into a knot with a radius of approximately 6 mm at the upper end. Roots were densely distributed in the upper soil layer and sparsely in the lower layer (*Liu, 2008*) (Fig. 2c). Under actual field conditions, wheat roots are tightly bonded to the soil, functioning to reinforce the soil structure. Wheat possesses a fibrous root system consisting of primary and secondary roots (Fig. 2b), with negligible differences in diameter and ultimate shear force between the two root types. Considering computational efficiency and simulation speed, primary and secondary roots were modeled as a single root type (*Guo, 2008*).

(a) Wheat root samples *(b) Morphological structure of wheat roots*

Fig. 2 - Wheat root system sample and morphological structure

Ten roots were randomly selected from each cluster to measure physical parameters. The average length, diameter, and mass of wheat roots were 87.2 mm, 0.31 mm, and 0.521 g, respectively, with a mass per unit length of 1.195×10^{-4} g/mm.

Due to the anisotropy and small diameter of wheat roots, constructing a DEM model capable of both bending and fracture is challenging, resulting in limited research in this area. Drawing on previous studies (Liu, 2018) and combining physical parameters of wheat roots, a wheat root model was established using rapid filling with particles of 0.15 mm in diameter. The Hertz-Mindlin with bonding contact model was selected for inter-particle interactions.

To calibrate the particle density for root model filling in DEM, the particle density was iteratively adjusted until the mass per unit length of the simulated root model matched that of actual roots, as described by Eq. (1). The calibrated particle density was 87.6 kg/m³.

$$\frac{m_R}{l_R} = \frac{m_r}{l_r} \tag{1}$$

where: m_R, m_r—mass of actual and simulated roots, g;

l_R, l_r—length of actual and simulated roots, mm.

Basic Physical Parameters of Soil

Soil samples were collected after wheat harvest, with an average bulk density of 1.41 g/cm³ and soil compaction of 2.88 MPa. To realistically simulate soil particle fracture and breakage, the Hertz-Mindlin with bonding contact model was adopted based on the soil type of the experimental field. Simulation time decreases geometrically with increasing soil particle radius. Referring to previous studies on soil-tool interactions, spherical soil particles with a radius of 8 mm were used (*Ucgul et al., 2017; Ding et al., 2017; Zheng et al., 2016*). Soil material and contact parameters were determined through experimental measurements and literature review (*Ding et al., 2018; Guo et al., 2017; Wang et al., 2017*), as presented in Table 1.

Table 1

Basic parameters of soil discrete element model

Parameter	Value
Soil density/(kg·m^{-3})	1410
Soil Poisson's ratio	0.4
Soil shear modulus/(Pa)	6×10^{7}
Inter-soil dynamic friction coefficient	0.4
Inter-soil static friction coefficient	0.34
Inter-soil restitution coefficient	0.6
Inter-soil bonding radius/(mm)	8.5
Inter-soil bonding stiffness/(N·m^{-3})	2.4×10^{6}
Inter-soil critical stress/(Pa)	235000

Establishment of Discrete Element Model and Parameter Calibration Method
Wheat Roots

Actual shear tests were conducted on wheat roots to measure the ultimate shear force at root breakage. A DEM model of wheat roots was then established for shear simulations, and the ultimate shear force of the simulated model was obtained. Full-level tests were performed on key model parameters using the actual root ultimate shear force as the target value to establish a response equation and calibrate the key parameters.

Actual Shear Test of Wheat Roots

Referring to relevant shear test standards (*Lenaerts et al., 2014; Yuan, 2019*), actual shear tests were conducted to measure the ultimate shear force of roots (Fig. 3a). To prevent root breakage and slippage at the clamping points during testing, custom fixtures were fabricated, and both ends of the roots were wrapped in 16 mm-thick sponges in their natural state. Twenty wheat roots with consistent length and diameter were sheared at a speed of 4 mm/s using a DDL10 universal testing machine. Sixteen samples where root breakage occurred at the midpoint were selected to ensure fracture was induced by the cutter rather than clamping forces. The average ultimate shear force at root breakage was 3.7 N, with the fracture position shown in Fig.3b.

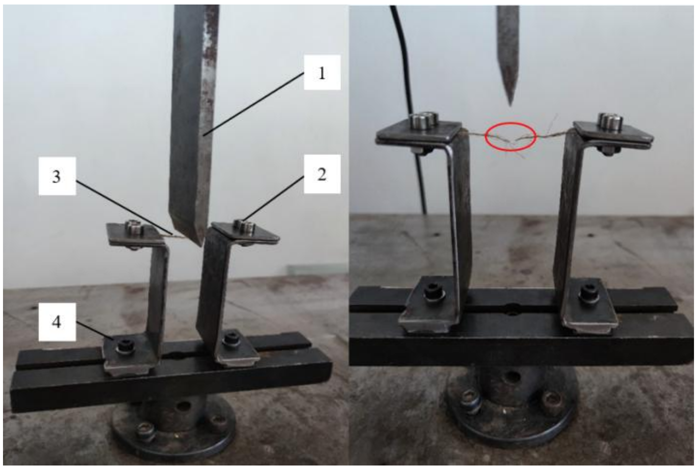

（a）Shear test *（b）Root fracture*

Fig. 3 - Actual root shear test

1.Cutter; 2.Custom fixture; 3.Wheat root; 4.Base

Simulation Model and Parameters of Wheat Roots

A DEM model of wheat roots consistent with the actual shear test was constructed in EDEM (Fig. 4). Assuming no relative sliding between root-filling particles, both static and dynamic friction coefficients between root particles were set to 1. The geometric models of the fixture and cutter were made of 65Mn steel. Material and contact parameters of wheat roots and 65Mn were determined through literature review (*Boac et al., 2014; Pan, 2012*). The density, Poisson's ratio, and shear modulus of 65Mn were 7865 kg/m³, 0.3, and 7.9×10^{11} MPa, respectively.

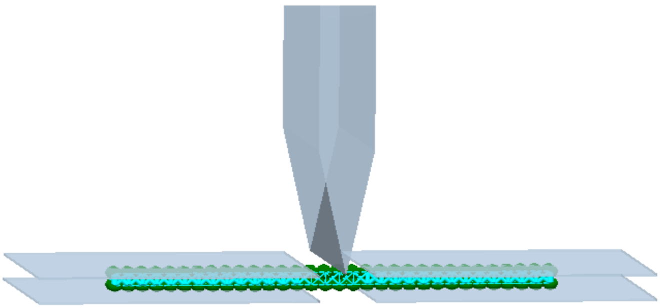

Fig. 4 - Shear simulation model

As determined earlier, the Hertz-Mindlin with bonding contact model was used for inter-particle interactions in wheat roots. Key parameters of this model include shear modulus, normal and tangential bonding stiffness, and bonding radius (*Ding et al., 2017; Zhang, 2012*). Since root-filling particles are randomly bonded, normal and tangential bonding parameters were set to be identical. Initial ranges of root particle model parameters were obtained through literature review and extensive shear simulation debugging, as listed in Table 2.

Table 2

Basic parameters of root model particles

Category	Simulation parameter	Value
Material parameters	Root density/(kg·m^{-3})	87.6
	Root Poisson's ratio	0.2-0.3a
	Root shear modulus/(MPa)	6-10a
Contact parameters	Root restitution coefficient	0.6-0.8a
	Root static friction coefficient	1
	Root dynamic friction coefficient	1
	Root-steel restitution coefficient	0.6-1a
	Root-steel static friction coefficient	0.35-0.6a
	Root-steel dynamic friction coefficient	0-0.02a
Bonding parameters	Bonding stiffness/(GN·m^{-3})	1-10a
	Critical stress/(MPa)	1-1.5a
	Bonding radius/(mm)	0.25-0.5a

Note: "a" indicates parameters to be screened.

Parameter Calibration Method for Wheat Root-Soil Complex Based on Ultimate Shear Force

Ultimate shear force is a key reference characteristic for calibrating WRSC models (*Yuan et al., 2020*). To obtain accurate contact and bonding parameters at the wheat root-soil interface, actual shear tests on WRSC were conducted following relevant literature methods (*Mak et al., 2012; Jiang et al., 2018; Zhao et al., 2019; Zheng et al., 2017*) to measure the ultimate shear force. Shear simulations of the WRSC model were then performed, and key parameters such as static and dynamic friction coefficients, bonding stiffness, and critical stress of the Hertz-Mindlin with bonding contact model at the root-soil interface were calibrated using the steepest ascent method.

Sampling of Wheat Root-Soil Complex

On the day after wheat harvest, areas with uniform soil conditions were selected in the middle of the field. Taking the center of wheat stubble as the sampling point, WRSC samples were collected using an uncovered iron box of 250 mm × 250 mm × 200 mm (Fig. 5a). The sampling process involved slowly driving the iron box into the soil with a hammer, excavating the soil around the box, and removing the box together with the WRSC. Sampling was repeated 8 times (Fig. 5b). To exclude the influence of stubble during modeling, above-ground stubble was cut off, retaining only the underlying wheat roots. The collected WRSC samples are shown in Fig. 5c. During storage and transportation, samples were wrapped in sponges to prevent fragmentation due to vibration.

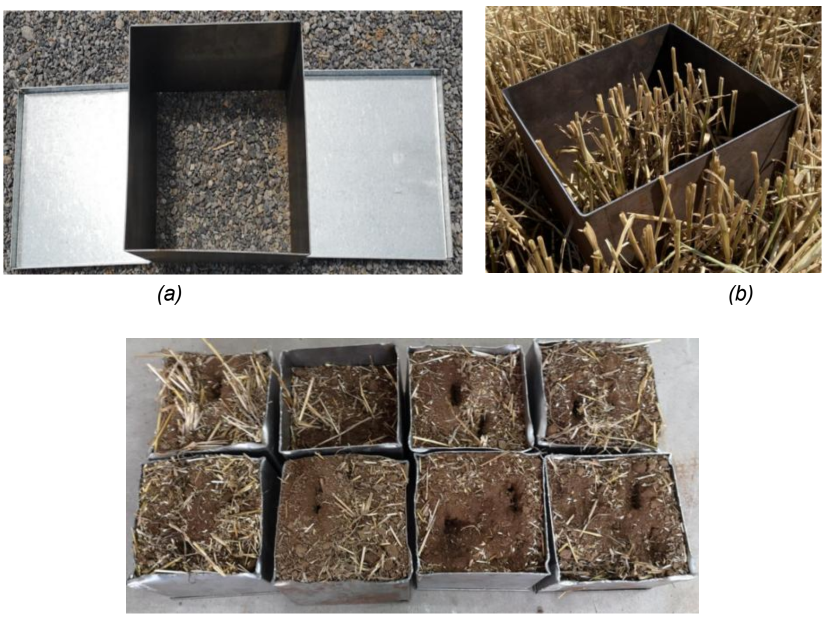

(a) *(b)*

(c)

Fig. 5 - Root-soil complex field sampling (b) with iron box (a) and the sample (c)

Sampling of Wheat Root-Soil Complex

Shear tests on WRSC samples were conducted using a universal testing machine in the mechanical laboratory (Fig. 6) to measure the ultimate shear force when the cutter sheared the midpoint of wheat roots. To prevent cutter deviation during shearing, the shear speed was set to 2 mm/s (*Liu, 2018*). Each shear test was repeated 8 times, and the average ultimate shear force was 445 N.

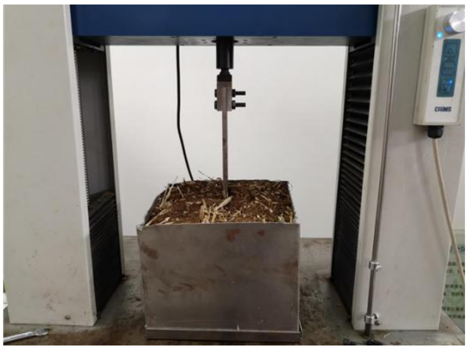

Fig. 6 - Shear test of root-soil complex

Previous studies by *Liu (2018)* and *Sun (2011)* indicated that friction and bonding forces between roots and soil are key factors contributing to the increased ultimate shear force of the complex. The Hertz-Mindlin with bonding contact model was therefore adopted for root-soil interactions. To reduce the number of parameters to be calibrated, the restitution coefficient and bonding stiffness at the root-soil interface were set to 0.6 and 1×10^7 N/m³, respectively, based on literature review (*Asaf et al., 2007; Zheng et al., 2016*). The bonding radius between wheat roots and soil was determined to be 4 mm through DEM simulation debugging.

RESULTS AND DISCUSSION

Calibration Test Results and Analysis of Wheat Roots

As shown in Table 2, 9 parameters need to be determined for wheat root shear simulations. However, the influence of each parameter on root shear resistance varies (*Liu et al., 2016*). To screen parameters with significant effects on the ultimate shear force of the root model, Plackett-Burman test design was performed using Design-Expert software. Significance analysis of the 9 undetermined parameters was conducted through root shear simulation tests. Each parameter was set at two levels (high and low), encoded as +1 and -1, respectively. According to Plackett-Burman test design requirements, 3 sets of zero-level tests were included, resulting in a total of 15 shear simulation tests with different parameter combinations. The shear speed was set to 4 mm/s. Test parameters, levels, and simulation results are presented in Tables 3 and 4, respectively.

Table 3

Placket-Burman test parameter list

Parameter	Parameter No.	Parameter level	
		Low level (-1)	High level (+1)
Root Poisson's ratio	X1	0.2	0.3
Root shear modulus/(MPa)	X2	6	10
Root restitution coefficient	X3	0.6	0.8
Root-steel restitution coefficient	X4	0.6	1
Root-steel static friction coefficient	X5	0.35	0.6
Root-steel dynamic friction coefficient	X6	0	0.02
Bonding stiffness/(GN·m⁻³)	X7	1	10
Critical stress/(MPa)	X8	1	1.5
Bonding radius/(mm)	X9	0.25	0.5

Table 4

Placket-Burman experimental design and results

No.	X_1	X_2	X_3	X_4	X_5	X_6	X_7	X_8	X_9	Ultimate shear force/(N)
1	0	0	0	0	0	0	0	0	0	4.956
2	1	1	1	-1	-1	-1	-1	-1	1	7.165
3	1	1	-1	1	1	1	-1	-1	-1	1.403
4	-1	1	1	1	-1	-1	-1	1	-1	1.347
5	-1	-1	-1	1	-1	1	1	-1	1	4.273
6	1	-1	1	1	1	-1	-1	-1	1	4.085
7	0	0	0	0	0	0	0	0	0	4.956
8	-1	-1	1	-1	1	1	-1	1	1	4.119

No.	X_1	X_2	X_3	X_4	X_5	X_6	X_7	X_8	X_9	Ultimate shear force/(N)
9	-1	1	-1	1	1	-1	1	1	1	9.069
10	0	0	0	0	0	0	0	0	0	4.956
11	1	-1	1	1	-1	1	1	1	-1	3.491
12	-1	-1	-1	-1	-1	-1	-1	-1	-1	1.362
13	1	1	-1	-1	-1	1	-1	1	1	3.795
14	1	-1		-1	1	-1	1	1	-1	2.889
15	-1	1	1	-1	1	1	1	-1	-1	2.888

Analysis of variance (ANOVA) of simulation results was performed using Design-Expert software, and the effects of each parameter on ultimate shear force are presented in Table 5. Bonding radius, bonding stiffness, and root shear modulus were found to have significant effects on ultimate shear force, while other parameters had minimal impacts. Therefore, only these three parameters were considered in subsequent steepest ascent and screening tests.

Table 5

Placket-Burman significance analysis of test parameters

Parameter	Parameter No.	Effect	Sum of squares	Influence rate/%	Significance ranking
Root Poisson's ratio	X1	-0.038	4.408×10-3	6.090×10-3	9
Root shear modulus/(MPa)	X2	0.91	2.47	4.07	3
Root restitution coefficient	X3	0.051	2.95	0.011	8
Root-steel restitution coefficient	X4	0.24	0.18	0.24	7
Root-steel static friction coefficient	X5	0.50	0.76	1.05	6
Root-steel dynamic friction coefficient	X6	-0.99	7.701×10-3	3.42	4
Bonding stiffness/(GN·m⁻³)	X7	2.28	15.56	21.49	2
Critical stress/(MPa)	X8	0.59	1.04	1.44	5
Bonding radius/(mm)	X9	3.19	30.48	42.11	1

To further narrow the ranges of root shear modulus (G), bonding stiffness (K), and bonding radius (Rb), steepest ascent tests were conducted. Subsequently, Box-Behnken tests were performed to establish a response equation through regression analysis of these three parameters. Taking the actual root ultimate shear force as the target value, the optimal values of G, K, and Rb were obtained using Design-Expert software. The factor levels and simulation results of the steepest ascent tests are presented in Table 6.

Table 6

Steepest climbing test and results

No.	Shear modulus G (X_2)/(MPa)	Bonding stiffness K (X_7)/(GN·m⁻³)	Bonding radius Rb (X_9)/(mm)	Ultimate shear force F_R/(N)	Relative error/%
1	6	2	0.25	1.86	49.73
2	7	4	0.3	3.34	9.73
3	8	6	0.35	4.48	21.08
4	9	8	0.4	5.21	41.81
5	10	10	0.45	7.27	96.49

As shown in Table 6, relatively small relative errors were observed at levels 2 and 3. These levels were therefore selected as the low (-1) and high (+1) levels for Box-Behnken tests. The factor levels, test design, and results are presented in Tables 7 and 8, respectively. Quadratic polynomial ANOVA of simulation results was performed using Design-Expert software.

Table7

Box-Behnken test factor level table

Factor	Level		
	Low (-1)	Medium (0)	High (+1)
Shear modulus/(MPa)	7	7.5	8
Bonding stiffness/(GN·m⁻³)	4	5	6
Bonding radius/(mm)	0.3	0.325	0.35

Table 8

Steepest climbing test and results

No.	Shear modulus/(MPa)	Bonding stiffness/(GN·m⁻³)	Bonding radius/(mm)	Ultimate shear force F_R/(N)
1	7.5	5	0.325	3.55
2	7.5	6	0.35	4.36
3	7.5	4	0.3	3.42
4	7	5	0.3	3.18
5	8	6	0.325	3.56
6	7	4	0.325	3.64
7	7.5	5	0.325	3.55
8	8	5	0.35	4.02
9	8	4	0.325	3.82
10	7	5	0.35	3.92
11	8	5	0.3	3.25
12	7.5	5	0.325	3.55
13	7.5	5	0.325	3.55
14	7.5	5	0.325	3.55
15	7.5	4	0.35	4.74
16	7.5	6	0.3	3.05
17	7	6	0.325	3.94

Non-significant terms were eliminated to optimize the regression model while ensuring model significance and non-significant lack of fit. The ANOVA results of the optimized model are presented in Table 9.

Table 9

The Box-Behnken results of quadratic polynomial variance analysis after experimental optimization

Source of variation	Sum of squares	Degrees of freedom	Mean square	P-value
Model	3.36	6	0.49	< 0.0001**
Shear modulus G	0.090	1	0.090	0.0196*
Bonding stiffness K	0.078	1	0.078	0.0269*
Bonding radius Rb	2.83	1	2.83	< 0.0001**
G×Rb	0.16	1	0.16	0.0047**
K²	0.062	1	0.062	0.0433*
Rb²	0.14	1	0.14	0.0071**
Residual	0.10	9	0.011	
Lack of fit	0.10	5	0.020	
Pure error	0.000	4	0.000	
Total	3.50	16		
Fit statistics: R^2=0.9711; Adjusted R^2=0.9486; Coefficient of variation (CV)=2.85%; Adequate precision=21.786				

Note: ** indicates extremely significant difference ($P < 0.01$); * indicates significant difference ($P < 0.05$).

As shown in Table 9, bonding radius (Rb), the interaction term of shear modulus and bonding radius (G×Rb), and the quadratic term of bonding radius (Rb^2) had extremely significant effects on the ultimate shear force of wheat roots. Shear modulus (G), bonding stiffness (K), and the quadratic term of bonding stiffness (K^2) had significant effects. The model exhibited high significance ($P < 0.01$), good reliability (CV=2.85%), excellent fit (R^2=0.9711, Adjusted R^2=0.9486 > 0.8), and high precision (adequate precision=21.786). The optimized regression equation is as follows:

$$F_R = 3.58 - 0.11 \times G + 0.60 \times R_b - 0.14 \times G \times K - 0.20 \times G \times R_b + 0.12 \times K^2 + 0.18 \times R_b^2 \quad (2)$$

To minimize the difference between simulated and actual ultimate shear forces of wheat roots, parameter optimization was performed using the optimization module of Design-Expert software. The optimal values were determined as follows: shear modulus of 7.96 MPa, bonding stiffness of 4.13 GN/m³, and bonding radius of 0.32 mm. Three repeated simulations were conducted with these optimal parameters, yielding ultimate shear forces of 3.725 N, 3.72 N, and 3.74 N, with relative errors of 0.68%, 0.54%, and 1.08%, respectively. The small relative errors indicate that the calibrated wheat root model exhibits shear resistance consistent with actual roots and can be used as a substitute for mechanical simulations.

Calibration Results and Analysis of Wheat Root-Soil Complex Parameters Based on Ultimate Shear Force

Establishment of the WRSC DEM model requires determining parameters such as static and rolling friction coefficients at the root-soil interface, as well as bonding stiffness, bonding stress, and bonding radius of the Hertz-Mindlin with bonding contact model. Based on the actual ultimate shear force of the WRSC, shear simulations of the WRSC model were performed to calibrate these key parameters (Fig. 7). The shear speed in simulations was consistent with that in actual tests. Referring to relevant literature (Lenaerts et al., 2014; Liu, 2018), the dynamic friction coefficient was set to 0.3. The effective ranges of the static friction coefficient, particle bonding stiffness, and particle bonding stress at the root-soil interface were determined as 0.3~0.9, 1~13 MN/m³, and 1~13 MPa, respectively.

Steepest ascent tests were conducted within the determined parameter ranges to simulate shear of the WRSC model. The factor levels and simulation results are presented in Table 10. At test No. 6, the shear resistance was 453 N with a relative error of 1.80% (< 5%). Thus, the calibrated parameters at the wheat root-soil interface were determined as follows: static friction coefficient of 0.8, bonding stiffness of 11 MN/m³, and critical stress of 11 MPa.

Table 10

Horizontal design of the steepest climbing test factors and shear simulation results

No.	Static friction coefficient f_{r-s}	Bonding stiffness τ_{r-s}/(MN·m^{-3})	Critical stress σ_{r-s}/(MPa)	Shear resistance/(N)	Relative error/%
1	0.3	1	1	322	27.64
2	0.4	3	3	346	22.25
3	0.5	5	5	361	18.88
4	0.6	7	7	383	13.93
5	0.7	9	9	410	7.87
6	0.8	11	11	453	1.80
7	0.9	13	13	506	13.71

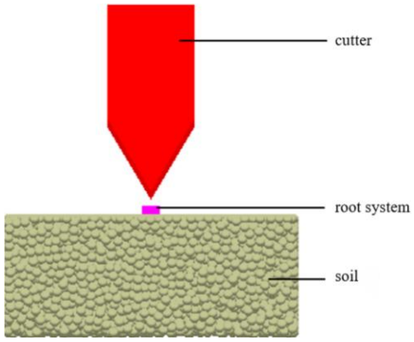

Fig. 7 - Shear simulation of root-soil complex

The calibrated static friction coefficient, bonding stiffness, and critical stress at the wheat root-soil interface were reconfigured in EDEM. Shear tests on the WRSC were then performed at the midpoint of wheat roots, and the cutter resistance-vertical displacement curve was exported after simulation (Fig. 8). The simulated shear resistance curve was found to be in good agreement with the actual curve. Within the depth range of 30-100 mm, the relative error between simulated and actual shear resistance was 7.32%, indicating that the calibrated WRSC DEM model can accurately simulate actual field soil conditions.

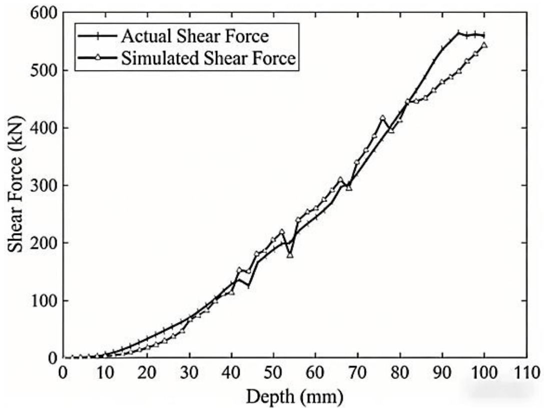

Fig. 8 - After parameter calibration, simulation and test cutter resistance-displacement curve

CONCLUSIONS

(1) A wheat root model was constructed using rapid particle filling and the Hertz-Mindlin with bonding contact model. Through Plackett-Burman screening tests and steepest ascent tests, inter-particle bonding radius, bonding stiffness, and particle shear modulus were identified as the significant parameters affecting the ultimate shear force of wheat roots. Using Box-Behnken design with ultimate shear force as the target value, the optimal parameters were calibrated as follows: root shear modulus of 7.96 MPa, inter-particle bonding stiffness of 4.13 GN/m³, and bonding radius of 0.32 mm.

(2) Actual and simulated shear tests were conducted on the WRSC. With the ultimate shear force on the cutter as the target value, key parameters at the root-soil interface were calibrated: static friction coefficient of 0.8, bonding stiffness of 11 MN/m³, and critical stress of 11 MPa.

(3) Validation of the WRSC model showed a relative error of 7.35% between the ultimate shear force of the calibrated model and the actual value, indicating that the DEM-based WRSC model can be used to simulate actual field soil environments.

REFERENCES

[1] Barr, J., Desbiolles, J., Ucgul, M., Fielke, J.M., (2020). Bentleg furrow opener performance analysis using the discrete element method. *Biosystems Engineering, Vol.* 189, pp. 99-115, United States.

[2] Barr, J.B., Desbiolles, J.M.A., Fielke, J.M., (2016). Minimising soil disturbance and reaction forces for high speed sowing using bentleg furrow openers. *Biosystems Engineering*, Vol. 151, pp. 53-64, USA.

[3] Chen, Y., Munkholm, L.J., Nyord, T., (2013). A discrete element model for soil–sweep interaction in three different soils. *Soil and Tillage Research*, Vol. 126, pp. 34-41, Netherlands.

[4] Chen W.Q., (2026). Analysis Of The Operational Performance Of Straw Baler Pickup Device Based On Edem And Adams. *INMATEH Agriculture Engineering*, Vol. 78, No. 1, Romania.

[5] Ding, S., Bai, L., Yao, Y., Yue, B., Fu, Z., Zheng, Z., Huang, Y., (2018). Discrete element modelling (DEM) of fertilizer dual-banding with adjustable rates. *Computers and Electronics in Agriculture*, Vol. 152, pp. 32-39, Netherlands.

[6] Hang, C., Gao, X., Yuan, M., Huang, Y., Zhu, R., (2018). Discrete element simulations and experiments of soil disturbance as affected by the tine spacing of subsoiler. *Biosystems Engineering*, Vol. 168, pp. 73-82, United States.

[7] Li, S.B., Huan, X.L., Wang, T.Y., (2024). Biomechanical properties and discrete element modeling of PSR stalks during silage harvest. *Computers and Electronics in Agriculture*, Vol.217: 108644, Netherlands.

[8] Solhjou, A., Desbiolles, J.M.A., Fielke, J.M., (2013). Soil translocation by narrow openers with various blade face geometries. *Biosystems Engineering*, Vol.114, pp. 259-266, United States.

[9] Solhjou, A., Fielke, J.M., Desbiolles, J.M.A., (2012). Soil translocation by narrow openers with various rake angles. *Biosystems Engineering*, Vol. 112, pp. 65-73, United States.

[10] Solhjou, A., Fielke, J.M., Desbiolles, J.M.A., Saunders, C., (2014). Soil translocation by narrow openers with various bent leg geometries. *Biosystems Engineering*, Vol. 127, pp. 41-49, United States.

[11] Tanaka, H., Momozu, M., Oida, A., Yamazaki, M., (2000). Simulation of soil deformation and resistance at bar penetration by the Distinct Element Method. *Journal of Terramechanics*, Vol. 37, pp. 41-56, UK.

[12] Ucgul, M., Fielke, J.M., Saunders, C., (2014). 3D DEM tillage simulation: Validation of a hysteretic spring (plastic) contact model for a sweep tool operating in a cohesionless soil. *Soil and Tillage Research*, Vol. 144, pp. 220-227, Netherlands.

[13] Yang, L., Wu,P, Zuo, Z.,(2024). E Roots: a three-dimensional dynamic growth model of rice roots coupled with soil. *Biosystems Engineering*, Vol. 244, pp. 122-133, United States.

[14] Cao, X.D., (2018). Structural optimization and experimental study of core share furrow opener (芯铧式开沟器结构优化及试验研究). *Northwest A&F University*, Yangling/China.

[15] Fang, H.M., Ji, C.Y., Chandio, F.A., Guo, J., Zhang, Q.Y., Arslan, C., (2016a). Discrete element method analysis of soil movement behavior during rotary tillage (基于离散元法的旋耕过程土壤运动行为分析). *Transactions of the Chinese Society for Agricultural Machinery*, Vol. 47, pp. 22-28, Beijing/China.

[16] Fang, H.M., Ji, C.Y., Tagar, A.A., Zhang, Q.Y., Guo, J., (2016b). Simulation analysis of straw displacement in straw-soil-rotary blade system (秸秆-土壤-旋耕刀系统中秸秆位移仿真分析). *Transactions of the Chinese Society for Agricultural Machinery*, Vol. 47, pp. 60-67 (in Chinese with English abstract).

[17] He, J., Li, H.W., Chen, H.T., Lu, C.Y., Wang, Q.J., (2018). Research progress on conservation tillage technologies and implements (保护性耕作技术与机具研究进展). *Transactions of the Chinese Society for Agricultural Machinery*, Vol. 49, pp. 1-19, Beijing/China.

[18] Huang, Y.X., Hang, C.G., Yuan, M.C., Wang, B.T., Zhu, R.X., (2016). Discrete element simulation and experiment of subsoiling soil disturbance behavior (深松土壤扰动行为的离散元仿真与试验). *Transactions of the Chinese Society for Agricultural Machinery*, Vol. 47, pp. 80-88, Beijing/China.

[19] Jia, H.L., Zheng, J.X., Yuan, H.F., Guo, M.Z., Wang, W.J., Jiang, X.M., (2017). Design and experiment of profiling sliding knife furrow opener (仿形滑刀式开沟器设计与试验). *Transactions of the Chinese Society of Agricultural Engineering*, Vol. 33, pp. 16-24, Beijing/China.

[20] Li, G.H., (2018). Structural design and experimental study of cross-slot furrow opener (十字槽开沟器结构设计及试验研究). *Northwest A&F University*, Yangling/China.

[21] Wang, X.Z., Yue, B., Gao, X.J., Zheng, Z.Q., Zhu, R.X., Huang, Y.X., (2018). Simulation and experiment of soil disturbance behavior with different wing shovel installation heights of subsoiler (深松铲不同翼铲安装高度时土壤扰动行为仿真与试验). *Transactions of the Chinese Society for Agricultural Machinery*, Vol. 49, pp. 124-136, Beijing/China.

[22] Yang, Y.L., (2015). Experimental study of core share furrow opener based on discrete element method (基于离散元法的芯铧式开沟器试验研究). *Jilin Agricultural University*, Changchun/China.

[23] Yu, J.Q., Qian, L.B., Yu, W.J., Pan, S.Q., Fang, Y., Fu, H., (2009). Discrete element method simulation analysis of furrow opener working resistance (开沟器工作阻力的离散元法仿真分析). *Transactions of the Chinese Society for Agricultural Machinery*, Vol. 40, pp. 53-57, Beijing/China.

[24] Zhai, L.X., Ji, C.Y., (2008). Establishment of soil mechanical contact model based on discrete element method (基于离散单元法的土壤力学接触模型的建立). *Jiangxi Agricultural Journal*, Vol. 20, pp. 108-111, Jiangxi/China.

[25] Zhang, J.C., Yan, X.L., Li, G.H., Cao, X.D., Liu, N., Sun, L.W., Tong, M., (2019). Design of cross-slot furrow opener for separate application of seed and fertilizer and stratified fertilization (十字槽种肥分施及分层施肥开沟器设计). *Journal of Agricultural Mechanization Research*, Vol. 41, pp. 86-90, Heilongjiang/China.

[26] Zhang, J.C., Yan, X.L., Lin, Z.K., Zhu, R.X., (2016). Design and experiment of self-excited vibration subsoiling and land preparation machine (自激式振动深松整地机设计与试验). *Transactions of the Chinese Society for Agricultural Machinery*, Vol. 47, pp. 44-49+72, Beijing/China.

[27] Zhao, S.H., Liu, H.J., Tan, H.W., Cao, X.Z., Zhang, X.M., Yang, Y.Q., (2017). Design and performance test of furrow opener imitating sailfish head curve (仿旗鱼头部曲线型开沟器设计与性能试验). *Transactions of the Chinese Society of Agricultural Engineering*, Vol. 33, pp. 32-39, Beijing/China.